



Power Electronic Systems
Laboratory

© 2012 IEEE

Proceedings of the International Conference of Integrated Power Electronics Systems (CIPS 2012), Nuremberg, Germany,
March 6-8, 2012

Design of a PCB Rogowski Coil Based on the PEEC Method

T. Guillod,
D. Gerber,
J. Biela,
A. Müsing

This material is published in order to provide access to research results of the Power Electronic Systems Laboratory / D-ITET / ETH Zurich. Internal or personal use of this material is permitted. However, permission to reprint/republish this material for advertising or promotional purposes or for creating new collective works for resale or redistribution must be obtained from the copyright holder. By choosing to view this document, you agree to all provisions of the copyright laws protecting it.



Eidgenössische Technische Hochschule Zürich
Swiss Federal Institute of Technology Zurich

Design of a PCB Rogowski Coil based on the PEEC Method

T. Guillod, D. Gerber and J. Biela
 Laboratory for High Power Electronic Systems
 ETH Zurich, Physikstrasse 3, 8092 Zurich, Switzerland
 Email: gerberdo@ethz.ch

A. Müsing
 Power Electronic Systems Laboratory
 ETH Zurich, Physikstrasse 3, 8092 Zurich, Switzerland
 Email: muesing@lem.ee.ethz.ch

Abstract

In order to measure currents with high di/dt , Rogowski coils are usually used. This work studies the design of a PCB coil by means of electromagnetic field simulation. The PEEC method has been used to extract the parameters of the equivalent circuit of the coil geometry. Different winding arrangements were analyzed with respect to measurement signal strength and noise immunity. The magnetic coupling between the current sensor and the busbar is investigated for the used test setup. Finally, a comparison of the PEEC simulation results with measurements, applying a 400 A current pulse concludes this paper. The results show that the PEEC method allows a simulation of the coil including the setup in which it is used with a reasonable computational effort.

I. Introduction

In order to measure currents with high di/dt , Rogowski coil current transducers are widely used for power electronic converters and pulsed power systems. The sensor is non-intrusive and provides galvanic insulation between the coil and the conductor. Furthermore, the transducer can measure large currents without saturation problems, due to the absence of a magnetic core. Because of these advantages, Rogowski coils are used in pulsed power systems, where very fast current pulses must be measured in a high voltage environment. Also, because of their capability to measure large pulsed currents, they are used to detect short circuits and over currents.

In [1], PCB Rogowski coils have been used to measure currents in IGBT modules. Since PCB Rogowski coils have a very small thickness, they can also be easily integrated in a press pack IGBT module setup as shown in figure 1.

For designing the coil and predicting the performance, different numeric methods can be applied: The most common method for designing a coil is to use Biot-Savart's law and integrate the flux through the windings. However, for more complex winding and conductor geometries, numerical field simulations are required. Finite Element Method (FEM) simulations are possible for a Rogowski coil with a small number of turns, but the computational cost is far too high for a coil with many turns. A FEM simulation of 10 windings on a compute server with two 2.93 GHz Intel Xeon X5670 processors and 36 GB RAM takes more than 24 h.

Another approach would be to simulate the conductor via FEM excluding the Rogowski coil in order to find the distribution of the magnetic field and then to compute the flux through the coil in a post-processing step as proposed in [2]. In that case, it would be possible to find the mutual inductance between the bus bar conductor and an idealized Rogowski coil. However, other effects as the coils self inductance and the winding capacitance are neglected in this approach. Especially in pulsed power applications, these effects are very important. Therefore, another method is required to investigate the coil characteristics.

In the case of press pack technology, the dimensions of the measurement coil are imposed by the IGBT size. Another

constraint is that the bus bar should have a low inductance in order to limit over voltages during turn off and to increase current rise times in pulsed power systems. A low inductive setup requires a small distance between the conducting elements to minimize the area enclosed by the current. Therefore, the distance between the coil and the conductor has to be very small (< 1 mm). A picture of the press pack stack and the Rogowski coil is shown in Fig. 1. Since the conductor/winding geometry is quite complex, it is not possible to use analytical models to predict the measurement performance of the coil. For a PCB coil, standard inductor formulas for the self-inductance and the first resonance frequency are not applicable. Therefore, an accurate numerical method is needed to find the magnetic coupling between the Rogowski coil and a conductor with arbitrary geometry.

In this paper, a new approach is presented using the Partial Element Equivalent Circuit (PEEC) method. This method allows the simulation of complex coil geometries, including inductive as well as capacitive effects. The bandwidth of the coil, measurement sensitivity as well as the susceptibility to disturbance currents flowing outside the coil can be predicted in an accurate way. Also, the shape of the measurement conductor can be included in the simulation. Therefore it is possible to simulate the complete system with reasonable computational cost. Simulating the whole assembly on a computer with a

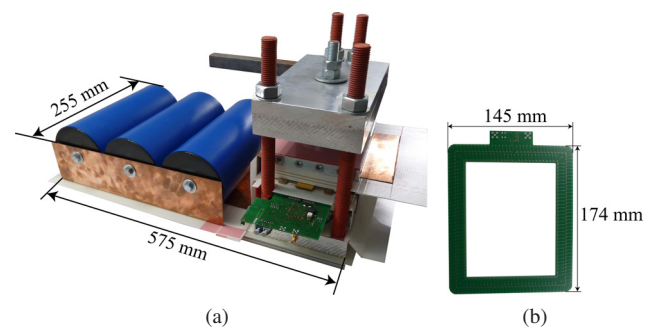


Fig. 1: Picture of (a) the press pack assembly (575x255x245 mm) and (b) the PCB Rogowski coil integrated in the press pack assembly.

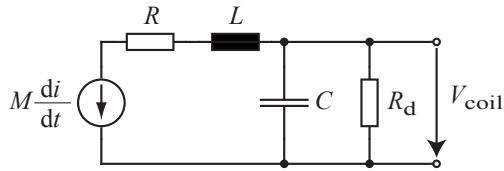


Fig. 2: Electrical model of a Rogowski coil valid up to the first resonance frequency. The distributed inductance and capacitances are summarized in two lumped components. R_d represents an additional external damping resistor.

Intel Core i5 3.1 GHz with 4 GB RAM takes approximately 15 min, which is significantly faster than the FEM simulation.

In the following, first a short overview over the Rogowski coil model and different winding arrangements is given. Then, the PEEC simulation is briefly introduced and the methods for extracting the coil's parameters are demonstrated. Finally, the complete hardware test setup is simulated, analyzed and compared with measurement results.

II. Model

In this section, the modeling of the coil is briefly introduced. Afterwards, the PEEC method is presented. Finally, the coil geometry is investigated by using the PEEC method and the results are discussed in detail.

A. Equivalent Circuit

The equivalent circuit for a Rogowski coil which is valid up to its first resonance frequency is shown in Fig. 2. The mutual inductance is modeled as a voltage source which represents the total induced voltage by the current to be measured. In order to model the high frequency behavior of the coil's self inductance, the parasitic winding capacitance as well as the total winding resistance is included in the model. In reality, all elements in this model are determined by spatially distributed inductors, capacitors and resistors and it would be physically more motivated to model each turn separately. However, it is sufficient to use the simplified model with only one voltage source, inductor, equivalent capacitor and resistor, because the coil is normally used below its first resonance frequency.

B. Transfer Function

By using the electrical model shown in Fig. 2, the transfer function of the coil is

$$G_{\text{coil}} = \frac{V_{\text{coil}}}{i} = \frac{s \cdot M}{L \cdot C \cdot s^2 + (R \cdot C + \frac{L}{R_d}) \cdot s + 1 + \frac{R}{R_d}} \cdot (1)$$

In most cases, the coil resistance can be neglected. Hence, the transfer function can be simplified to

$$G_{\text{coil}} = \frac{V_{\text{coil}}}{i} = \frac{s \cdot M}{L \cdot C \cdot s^2 + \frac{L}{R_d} \cdot s + 1} \cdot (2)$$

The transfer function indicates, that the coil voltage is proportional to the di/dt . To reconstruct the measured current, the output voltage of the coil has to be integrated over time, since the coil is only measures the di/dt .

The transfer function has a second order term in the denominator. Without damping resistor, the transfer function shows a resonance peak at the frequency $\omega_0 = \frac{1}{\sqrt{L \cdot C}}$. If pulse currents are measured, the resonance causes an overshoot in

the integrated output signal. Since the presented coil is used to detect over-currents in press pack IGBTs, an overshoot might cause an over-current detection to turn off the switch even if the real current is still at a safe level. Therefore, an appropriate damping of the coil is essential.

C. Mutual Inductance

During the design process, two important coil properties have to be considered. The first one is the measurement accuracy depending on the conductor's position within the Rogowski coil area. The second one is the magnetic coupling between the measured current and the coil. By using an analytical model as presented in [3] and [4], the measurement error depending on the current carrying conductor position can be calculated with analytical formulas.

Basically, the mutual inductance of every single turn to an infinitely thin conductor at a certain position \mathbf{r}_c is calculated by using Biot-Savart's law. Usually, the origin of the coordinate system is the center of the coil. Afterwards, the total mutual inductance $M(\mathbf{r}_c)$ is computed by summing the mutual inductances of the single turns. The measurement error depending on the position of the conductor is defined as follows:

$$\text{Error (\%)} = \begin{cases} 100 \cdot \left| 1 - \frac{M(\mathbf{r}_c)}{M_0} \right| & \text{inside the coil} \\ 100 \cdot \left| \frac{M(\mathbf{r}_c)}{M_0} \right| & \text{outside the coil} \end{cases} \quad (3)$$

Where M_0 is the mutual inductance for a conductor placed at the center of the coil.

In Fig. 3, the calculated measurement error depending on the conductor position is shown for the realized coil. The winding density is increased in the corners which leads to a significant reduction of the error close to the corners.

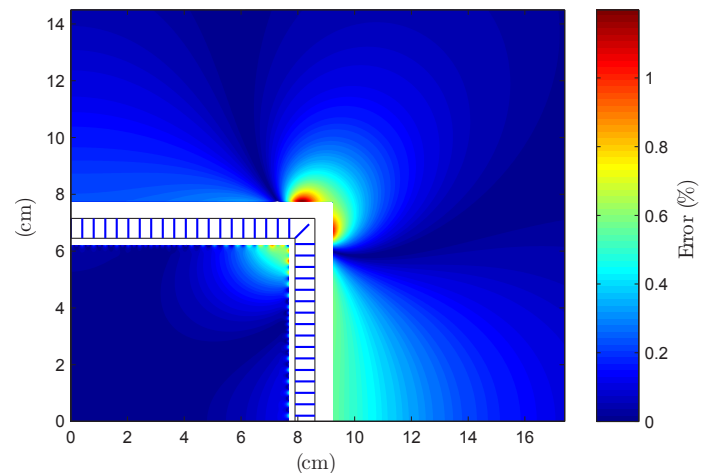


Fig. 3: Relative error depending on the position of the current for indefinitely long conductor perpendicular to the coil.

However, this simple model is very limited, since it is only possible to calculate the mutual inductance for each turn for an infinitely long conductor perpendicular to the coil at a certain position inside or outside the coil. Therefore, it can only be used to investigate the placement of the turns. To perform a more detailed investigation of the measurement behavior a better method has to be used which will be described in section II-F.

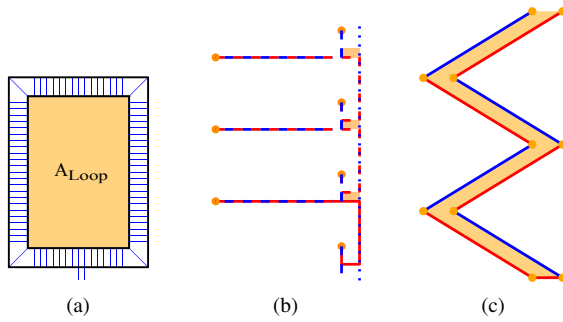


Fig. 4: Disturbance area for different compensation methods: (a) without compensation, (b) reduction of the disturbance area by using a return wire, (c) compensation of the disturbance area.

D. Damping

In order to avoid an overshoot of the measured signal, it has to be damped. If the coil signal is integrated with an ideal integrator, the transfer-function is a second order system which can be written in a general form:

$$G(s) = K \cdot \frac{\omega_0^2}{s^2 + 2 \cdot \zeta \cdot \omega_0 \cdot s + \omega_0^2} \quad (4)$$

Therefore, the optimal value for the damping resistor R_d can be calculated as

$$R_d = \frac{1}{2 \cdot \zeta} \cdot \sqrt{\frac{L}{C}} = \frac{1}{\zeta} \cdot \pi \cdot L \cdot f_{res}. \quad (5)$$

Critical damping is achieved for $\zeta = 1$. If a lower ζ is chosen, the rise time of the output signal is decreased, but there will also be an overshoot.

E. Disturbance Compensation

For currents not perpendicular to the plane A_{Loop} , the induced voltage can be very large since the coil itself is one big turn in this case. The area A_{Loop} of the coil shown in Fig. 4(a) is 25230 mm^2 which is much bigger than the total area enclosed by all turns (1635 mm^2). Hence, a compensation is required. Otherwise the noise immunity of the coil is very poor.

There are two different compensation methods. The first one is using a return wire from the endpoint of the coil back to the starting point (Fig. 4(b)). This reduces the disturbance area to 73 mm^2 . The second method is by continuing the turns at the end of the coil back to the starting point along the same path (Fig. 4(c)). In that case, the area is reduced to 1400 mm^2 . The different winding structures are shown in Fig. 5.

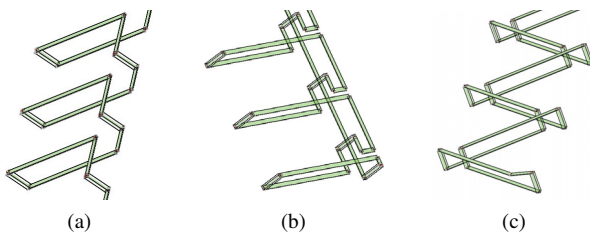


Fig. 5: Different winding structures: (a) without reduction mechanism, (b) with a return wire and (c) a bifilar winding.

F. PEEC Simulation

As previously mentioned, analytic methods are not suitable for complex geometries. In order to extract the coil's parameters like the resonance frequency, the self inductance and the distributed capacitance, the PEEC method has been used. Additionally, the test setup shown in Fig. 1 has been simulated to determine the measurement behavior of the coil.

1) PEEC Method

The simulations in this work use a PEEC-based simulation tool called GeckoEMC [5]. The PEEC method itself was originally derived for the EM modeling of IC interconnections. It is based on the discretization (meshing) of electrical conductors into partial elements i.e. inductors, capacitors, resistors, and voltage/current sources. Thus, it can be easily coupled to any circuit simulator as e.g. SPICE or GeckoCIRCUITS [6] and solved both in the time and frequency domain. In comparison to the FEM approach, the discretization of the surrounding air volume is not required and only the mesh of conductors and dielectrics has to be performed. Accordingly, the PEEC method turns out to be a fast and accurate modeling approach for the circuit-field coupled problems such as PCB tracks [7] and Rogowski coils.

PEEC discretizes conductors into many discrete partial elements as indicated in Fig. 6. The PEEC solver creates matrices of partial inductances $L_{p,ij}$, partial coefficients of potential $P_{ij} = C^{-1}$ and node resistances R_L . From this, a circuit equation system is generated and solved subsequently.

When retardation effects due to the finite speed c of light are included into the solution matrices as a complex phase shift, PEEC gives a full wave solution of the electrical field integral equation [8]–[10]. Other high frequency effects like skin and proximity effects are also included when the conductor geometry is subdivided into a finer mesh. However, this refinement increases the model size substantially. Therefore, the conductors for the Rogowski coil are modeled as cells without subdivision and thus neglecting the finite speed of light (quasi-static approximation) for simulation performance reasons.

The inclusion of dielectric PEEC volume cells such as required by the FR4 PCB material is generally possible [11]. However, an appropriate global relative permittivity was used which is derived from the FR4 permittivity. This approach helps to keep the total model size moderate, since then dielectric cells can be omitted from the model.

2) Coil Impedance

A PEEC model including conductors passing through a dielectric leads to a very large number of cells which increases the computational effort. A way to keep the number of cells low is to model the whole space filled with dielectric and to choose an appropriate global relative permittivity to simulate the coil impedance.

The turns of the coil can be treated as a coplanar stripline. The impedance calculation for coplanar striplines is described in [12]. There, an equivalent relative permittivity ϵ_{eff} is calculated depending on the waveguide structure.

$$\epsilon_{eff} = 1 + q \cdot (\epsilon_r - 1) \quad (6)$$

where ϵ_r is the relative permittivity of the PCB and q is the filling factor of the dielectric. For an infinitely thick dielectric,

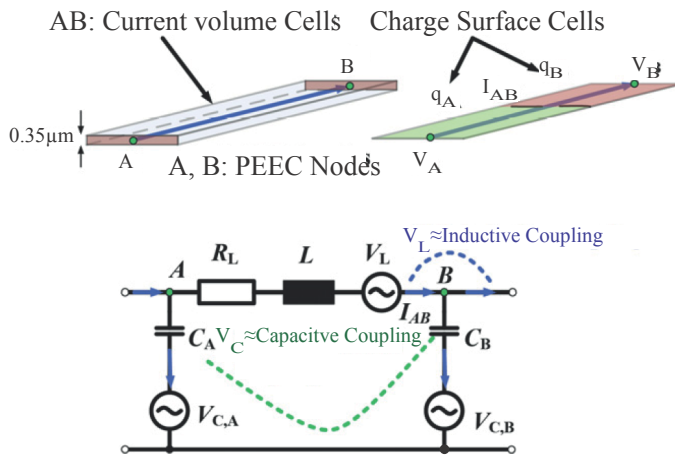


Fig. 6: PEEC-based modeling example: 0.35 μm PCB copper track.

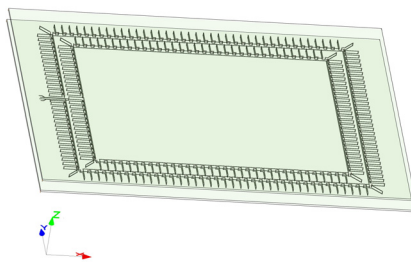


Fig. 7: Picture of the model used to extract the coil parameters

$q = 0.5$. For a PCB thickness of 1.6 mm, the value of q varies between 0.4 and 0.5 for a distance between the traces below 4 mm. A q value of 0.5 has been chosen for the simulation with PEEC which leads to an ϵ_{eff} of 2.75 for the FR4 permittivity ϵ_r of 4.5.

In PEEC, the definition of a ground node is required. To increase the stability of the solutions, the coil has been placed between two ground planes Fig. 7. In order to measure/extract the impedance, a current source was placed between the coil's terminals and the voltage across the source was measured. Since the wire skin effect has no influence on the resonance frequency, it was not taken into account.

To compare the different compensation methods as mentioned before, the self-inductance and the resonance frequency has been investigated. The mutual inductance for all coils is the same.

Table I shows the simulation results. The self-inductance is approximately the same for all three coils. The coil without any compensation a) shows the highest resonance frequency. The absence of any compensation leads to the shortest total trace length and therefore to the lowest distributed capacitance. The coil with bifilar turns c) has a slightly higher resonance

Geometry	L (μH)	f_{res} (MHz)
(a)	2.105	50.0
(b)	2.369	29.95
(c)	1.849	31.3

TABLE I: Comparison between different windings geometries for the self-inductance and first resonance frequency.

Conductor geometry	Winding geometry		
	(a)	(b)	(c)
(i) Analytical Calculation	3.462 nH	3.462 nH	-
(ii)	3.450 nH	3.453 nH	3.359 nH
(iii)	0.092 nH	0.094 nH	0.089 nH
(iv)	22.940 nH	0.087 nH	1.166 nH
(v)	1.193 nH	1.192 nH	1.191 nH

TABLE II: Comparison of the mutual inductance between different windings geometries for different current conductors. The direction of the current is labeled in red.

frequency as the coil with return wire b) which can be explained by the lower self-inductance.

3) Mutual Inductance

The PEEC method allows to simulate the interaction between a current flowing through a conductor and the coil. Hence, it is possible to determine the mutual inductance for the ideal case. Additionally, different conductor geometries can be simulated to investigate the noise immunity. The simulation results for different geometries for each compensation method are shown in Table II. The bars represent the current carrying conductor. The direction of the conductor is labeled in red. Here, capacitive effects were not taken into account.

The simulation results show a very good agreement between the analytical calculation and the simulation. Also, the noise immunity for the cases (iii) to (v) do not depend on the compensation mechanism except for case (iv). There, the mutual inductance for the coil without compensation is much bigger than the mutual inductance for case (ii). Therefore, this geometry is very sensitive to external magnetic fields and can only be used in an environment where external interferences are small.

The coil with a return conductor b) has the best noise immunity with only a slightly lower bandwidth than the coil c). To verify the simulations, the coil with b) has been built and the verification is presented in the following section.

III. Results

To verify the simulated results obtained with PEEC, certain measurements were made with a built coil. First, the coil's impedance was measured with a network analyzer. Then, a test

setup including the coil and a press pack IGBT is introduced and simulated with PEEC. Finally, the measurements with the Rogowski coil combined with the results of the PEEC Simulation are compared with a commercially available sensor.

A. Verification

The coil parameters of the built coil were measured with a network analyzer. The measured coil impedance and the simulated coil impedance are compared in Fig. 8.

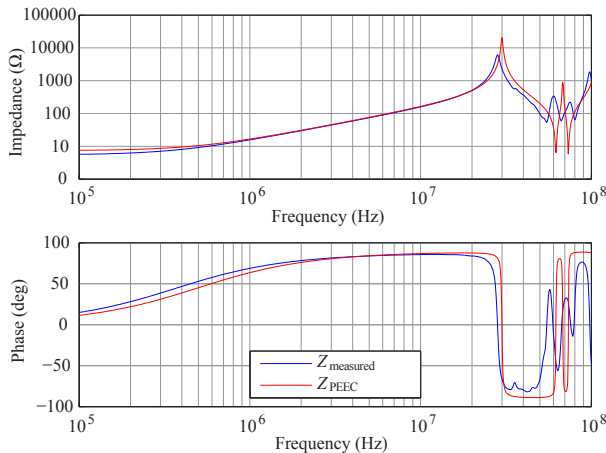


Fig. 8: Comparison between the measured coil impedance and the PEEC simulation.

The measured impedance shows a good agreement with the simulated curve up to the first resonance frequency. The deviation of the measured and the simulated impedance may have several reasons. First, the skin effect was not included in the simulation. Second, the model is based on a global permittivity which is not the case in the real system. Also, the frequency dependence of the permittivity of FR4 is not part of the model as well as the finite speed of light.

The influence of the skin effect at the simulated frequencies is low. The calculated global permittivity might not be accurate enough as the difference of the first resonance frequency between simulation and measurement shows. The frequency dependence of the FR4 strongly depends on the material used by the PCB manufacturer, but in general it starts to decay significantly at frequencies of a few ten MHz. To justify in which manner the effects mentioned before influence the impedance would require a detailed analysis of the used material which is not necessary in the case for which the coil is used.

The speed of light has an influence at the simulated frequencies since the coil has many turns. The total conductor length for the used coil is 3.75 m. It has to be considered that the speed of light in a dielectric is significantly lower than in vacuum. In that case, the wavelength of a traveling wave along the conductor is easily in the range of the conductor's length for frequencies of a few ten MHz. The wavelength at 10 MHz is 14 m, at 50 MHz it is already 2.8 m.

The simulated and measured coil parameters are shown in Table III. The measured capacitance was calculated out of the resonance frequency and the measured inductance.

The relative error for the inductance calculation is 1.2%. The resonance frequency is deviating by 6.2% since it strongly depends on the relative global permittivity ϵ_{eff} and the grounding of the dielectric. The relative error of the capacitance

	L (μH)	C (pF)	f_{res} (MHz)
PEEC Simulation	2.369	11.92	29.95
Measurement	2.34	13.61	28.2

TABLE III: Simulated and measured coil parameters

is 12% because it strongly depends on the resonance frequency and is not directly measured.

B. Test Setup

To predict the measurement response, the realized coil was further examined by simulating the coil and the press pack assembly (Fig. 9). The assembly consists of a press pack IGBT, diodes, a load resistor and several capacitors. The components are connected with copper busbars. The IGBT chips are modeled as cylindrical PEEC cells.

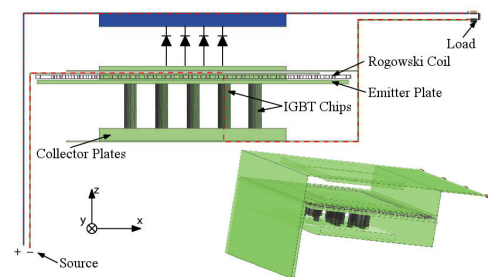


Fig. 9: Busbar geometry with the IGBT and the Rogowski coil (violet) at the emitter side. The current path is labeled in red.

The coil can be placed either at the emitter or the collector level. Since the gate driver and the integrator circuit are at emitter potential, the coil is placed at the emitter which simplifies the insulation of the coil. Also, the collector potential is changing during the turn on and turn off process with respect to the emitter potential. Therefore, the coil would be exposed to a large dV/dt . This, in turn, leads to disturbances of the coil output signal because the coil and the collector are capacitively coupled.

Since the test assembly is a low inductive design, the copper busbars are in close proximity to the Rogowski coil (case (v) in Table II). Therefore, the mutual inductance in the test setup will be higher than in the ideal case. The simulation of the mutual inductance of the coil in the test setup results in a mutual inductance of 3.78 nH which is 10% higher compared to an infinitely long wire.

The capacitive coupling between the busbar and the coil has to be included in the simulation. Therefore, the setup is simulated with inductive and capacitive coupling.

In Fig. 10, the ideal transfer function ($G_{\text{coil,ideal}}$) is compared with the transfer function of the equivalent circuit (G_{coil}) and the simulated transfer function ($G_{\text{coil,PEEC}}$). The coil was damped with $\zeta = 1$. The results show the validity of the equivalent circuit up to a frequency of 35 MHz. At higher frequencies, additional resonance frequencies appear which are not included in the equivalent circuit. The peak at 65 MHz is caused by a resonance in the busbar which also appears in the coil's transfer function due to the capacitive coupling.

C. Measurements

To verify the simulation results, the coil has been tested with a pulse current of 400 A and a pulse length of 4 μs .

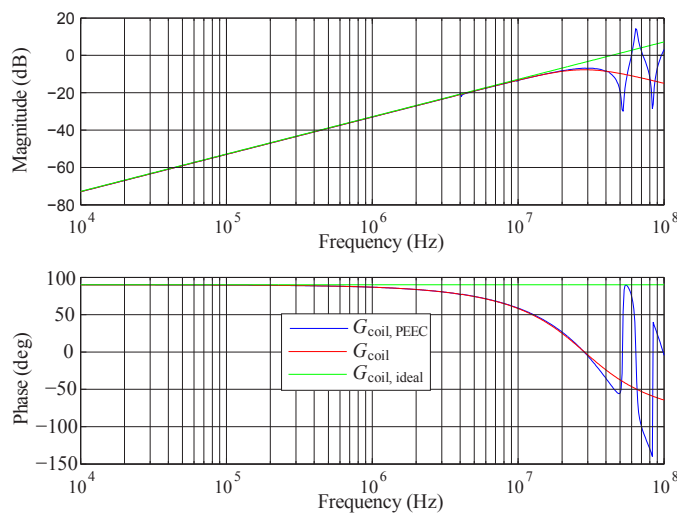


Fig. 10: Comparison of the transfer functions computed from fields simulation and from the equivalent circuit.

Additionally, the current through the load has been measured with a commercially available Rogowski coil (PEM CWT 60R).

To compare the measured coil signal with the commercially available sensor, the simulated transfer function was inverted in order to reconstruct the current out of the measured coil signal. The results are shown in Fig. 11. The predicted and the measured waveform match quite good. They show only a deviation of 2% at the end of the pulse rise. The current measured with the PEM CWT 60R shows a negative current at the beginning of the pulse which can be explained by parasitic capacitances at the load side. The bandwidth of the commercially available sensor (16 MHz) is lower than the PCB Rogowski coil bandwidth. This might be an explanation for the deviation of the oscillations at the beginning and at the end of the pulse since their frequency is almost the same as the sensor's bandwidth. Also, the currents are not measured at the same spatial position which could lead to an additional small variation between the two signals.

IV. Conclusion

In this paper, the PEEC method was used to investigate the design of a Rogowski coil. The simulation was used to extract the dominant coil parameters including the self inductance and the distributed winding capacitance.

The simulation results were compared with measurements performed with a network analyzer. The measurements showed a good match between the parameters extracted by the simulation and the measured parameters.

Also, it has been shown that it is possible to simulate a PCB Rogowski coil including the assembly by using the PEEC method with low computational effort compared to a FEM simulation. To verify the simulation results, the coil voltage was measured for a given current pulse. Afterwards, the current was extracted by using the simulated transfer function of the PEEC simulation and the measured coil voltage. The predicted current was compared with a measurement of the same pulse performed with a commercially available Rogowski coil. The results showed a good agreement between extracted and the measured current.

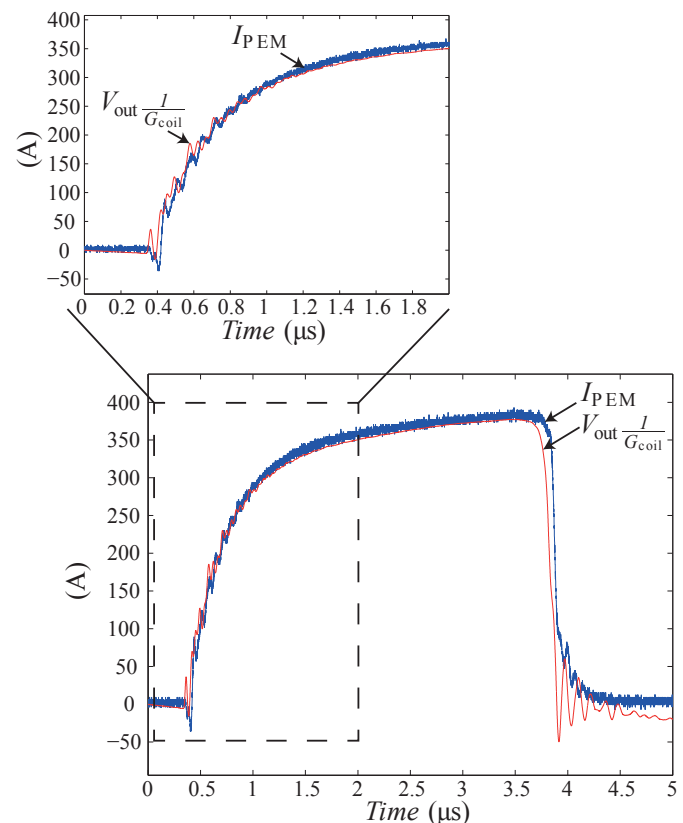


Fig. 11: PEEC simulation of a 400 A pulse with the measured PCB coil voltage as simulation input (red curves) compared with the PEM CWT 60R measurement (blue curves).

References

- [1] D. Bortis, J. Biela and J. Kolar, "Active gate control for current balancing in parallel connected IGBT modules in solid state modulators" in *Proc. of the 16th IEEE International Pulsed Power Conference*, vol. 2, pp. 1323–1326, June 2007.
- [2] M. Marracci, B. Tellini and C. Zappacosta, "FEM Analysis of Rogowski coils coupled with bar conductors" in *XIX IMEKO World Congress 2009, Fundamental and Applied Metrology*, Sept. 2009.
- [3] N. Karrer, P. Hofer-Noser and D. Henrard, "HOKA: a new isolated current measuring principle and its features" in *Proc. of the 34th IAS Annual Meeting Industry Applications Conf.*, vol. 3, pp. 2121–2128, 1999.
- [4] N. E. Karrer, *Hochdynamische Erfassung elektrischer Ströme über stossfrei verkoppelte Wandler*. VDI Verlag, 2002. Diss. ETH Zurich, Nr. 14332.
- [5] <http://www.gecko-research.com/geckoemc.html>.
- [6] <http://www.gecko-research.com/geckocircuits.html>.
- [7] A. Müsing, C. Zingerli, P. Imoberdorf and J. W. Kolar, "PEEC-based numerical optimization of compact radial position sensors for active magnetic bearings" in *Proc. of the 5th International Conference on Integrated Power Electronics Systems (CIPS '08)*, March 2008.
- [8] H. Heeb and H. Rueli, "Three-dimensional interconnect analysis using partial element equivalent circuits" *IEEE Trans. on Circuits and Systems I: Fundamental Theory and Applications*, vol. 39, no. 11, pp. 974–982, 1992.
- [9] J. Ekman, *Electromagnetic Modeling Using the Partial Element Equivalent Circuit Method*. PhD thesis, Lulea University of Technology, Mar. 2003. http://staff.ltu.se/~jekman/J_Ekman_PhDThesis.pdf.
- [10] A. E. Rueli, "Equivalent circuit models for three-dimensional multiconductor systems" *IEEE Transactions on Microwave Theory and Techniques*, vol. 22, no. 3, pp. 216–221, 1974.
- [11] A. E. Rueli and H. Heeb, "Circuit models for three-dimensional geometries including dielectrics" *IEEE Transactions on Microwave Theory and Techniques*, vol. 40, pp. 1507–1516, July 1992.
- [12] R. Simons, *Coplanar waveguide circuits, components, and systems*. Wiley series in microwave and optical engineering, Wiley-Interscience, 2001.